The effect of age on experimental animals during toxicological experiments is one of the interesting factors associated with toxicological endpoints. Two groups of linear configurations represented by five mice each for the 2-month-old and 21-month-old groups are shown in Figure 3.8a. These two different age groups show different expression diversities; the aged group (21 months old) shows a much wider range of expression intensities than the younger (2 months old) group. Furthermore, the order of gene expression intensity between the two groups is reversed. The wider expression intensities of the aged group suggest that senescent changes appear stochastically and are probabilistically different from one individual to another. Note that the wider expression intensities do not indicate differences in the quality of individual animals but the different probabilistic responses of individual animals during aging. These individual differences are also observed at the cellular level, if each cellular function is affected by gene expression (Bahar *et al.*, 2006).

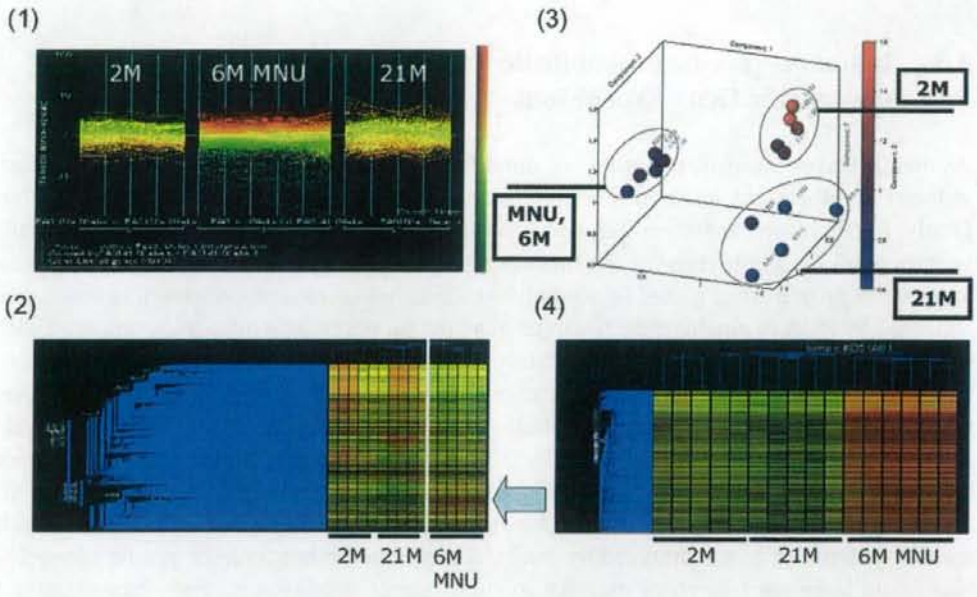

Figure 3.8 *(a) Age-related gene expression profiles determined from the bone marrow of 2-month-old and 21-month-old mice are shown in the line configuration. See text. (Six gene expression profiles of bone marrow obtained from mice 6 months after treatment with a single dose of methyl-nitroso-urea (MNU) at 50 mg kg^{-1} b.w.) (b) Two-dimensional dendrographic diagram of the same expressed genes from the bone marrow of 2-month-old and 21-month-old mice. (Six gene expression profiles of bone marrow obtained from mice 6 months after treatment with a single dose of MNU. Arrow indicates the gene cluster specifically up-regulated in the MNU-treated groups; an expanded view of the profiles is shown in (d).) (c) PCA of age control group, five mice each for the 2-month-old and 21-month-old groups, is shown in the three-dimensional contribution scores for components #1, #2 and #3, which discriminate between the clusters from the 2-month-old and 21-month-old groups. Six gene expression profiles of bone marrow obtained from mice 6 months after MNU treatment belong to another separate cluster. (d) Expanded view of profiles indicated by the arrow in (b) showing the gene cluster specifically up-regulated in the MNU-treated groups.*

Such differences between the two age groups cannot be defined using a dendrogram, as observed in the 10 columns on the left of Figure 3.8b, in which the aged group and the young group are not clearly separated. The reason that these different age groups are not clearly separated in the dendrogram is because of the relatively small number of genes with weak expressions that may define these different age groups. To pinpoint the possible responsible genes that define both groups, PCA was applied. Results show that there are discriminant components defined by components #1, #2 and #3, as shown in Figure 3.8c.

When one compares the gene expression profiles of these two age groups with those of mice treated with methyl-nitrosourea (MNU), a direct genophilic leukemogenic compound, the expression profiles of six bone marrow tissues from MNU-treated mice are clearly defined in the six columns on the right in Figure 3.8d. The discrimination of the clusters shown in the three-dimensional expressions is clearly separated in Figure 3.8c. The genes responsible for these discriminations can be autogenerated (data not shown).

3.8 Radiation-specific Probabilistic Union Genes after Subtracting Age-specific Gene Expressions

As mentioned previously, regardless of the difference between spontaneous and radiation-induced myelogenous leukemias, it took nearly a lifetime for both leukemias to develop fatally. Furthermore, radiation-induced myelogenous leukemias express stochastically divergent profiles, as observed in the line configuration in Figure 3.5. Therefore, each gene expression profile from a total of six radiation-induced myelogenous leukemia cases was analyzed by PCA to elucidate each unique gene list for nontreated mice and compared with the gene expression profiles of bone marrow cells from five 21-month-old nontreated mice. To obtain the union gene list, the gene expression profile of the 21-month-old group was compared separately with each individual expression profile of radiation-induced myelogenous leukemias by PCA followed by the selection of genes with a contribution score of over 1.0 from components #2 or #3 and #6 from the result of PCA (Table 3.1). In this PCA, the 287 union genes obtained were subtracted by 45 genes that overlapped with another 249 union genes analyzed by the PCA combination between the profile of the 21-month-old bone marrow group and that of spontaneous myelogenous leukemias (data not shown). Consequently, the final number of union genes obtained was 128 genes after the subtraction of 114 expression sequence tags (ESTs), which were generated in an unsupervised manner; however, most of them showed gene functions consistent with the response to radiation exposure. Specifically, five radiation-damage-related genes, including *Hus1*, *Eef1a2*, *Vegfc*, 13 cell cycle/cell-growth-related genes, and 12 apoptosis/cell-death-related genes were observed. Notably, 42 tumorigenesis-related genes (i.e. 33 %) were observed in which the down-regulation of tumor suppressor genes and the up-regulation of tumor promoter genes were commonly observed. The expressions of genes for cytoskeleton and cell adhesion molecules and those of genes for oxidative stress and inflammatory cytokines were also observed and included in the list; the expressions of these genes are also considered consequences of the xenobiotic responses to radiation exposure, because these genes were not included in the list of genes associated with spontaneous myelogenous leukemia (data not shown). As a reference to the functions of the autogenerated genes,

Table 3.1 *Union gene list for radiation-induced leukemias*

Affymetrix systemic name		Common name	Genbank ID	Description
1415874_at		*Spry1*	NM_011896	sprouty homolog 1 (*Drosophila*)
1416001_a_at		*Cotl1*	NM_028071	coactosin-like 1 (*Dictyostelium*)
1417097_at		*Nrbf1*	NM_025297	nuclear receptor binding factor 1
1417194_at		*Sod2*	NM_013671	superoxide dismutase 2, mitochondrial
1417602_at		*Per2*	AF035830	period homolog 2 (*Drosophila*)
1417623_at	*	*Slc12a2*	BG069505	solute carrier family 12, member 2
1417851_at		*Cxcl13*	AF030636	chemokine (C–X–C motif) ligand 13
1418062_at		*Eef1a2*	NM_007906	eukaryotic translation elongation factor 1 alpha 2
1418094_s_at		*Car4*	NM_007607	carbonic anhydrase 4
1418450_at		*Islr*	NM_012043	immunoglobulin superfamily containing leucine-rich repeat
1418547_at		*Tfpi2*	NM_009364	tissue factor pathway inhibitor 2
1418597_at		*Top3a*	NM_009410	topoisomerase (DNA) III alpha
1418666_at		*Ptx3*	NM_008987	pentaxin related gene
1418697_at	*	*Temt*	NM_009349	thioether *S*-methyltransferase
1418712_at		*Cdc42ep5*	NM_021454	CDC42 effector protein (Rho GTPase binding) 5
1418713_at		*Pcbd*	NM_025273	6-pyruvoyl-tetrahydropterin synthase/dimerization cofactor of hepatocyte nuclear factor 1 alpha (TCF1)
1418764_a_at		*Bpnt1*	BB412311	bisphosphate 3′-nucleotidase 1, metal-dependent lithium-inhibited phosphomonoesterase protein family
1419196_at		*Hamp1/Hepc*	NM_032541	hepcidin antimicrobial peptide
1419353_at		*Dpm1*	NM_010072	dolichol-phosphate (beta-D) mannosyltransferase 1
1419365_at		*Pex11a*	NM_011068	adaptor-related protein complex 3, sigma 2 subunit
1419417_at		*Vegfc*	NM_009506	vascular endothelial growth factor C
1419561_at	*	*Ccl3*	NM_011337	chemokine (C–C motif) ligand 3

Table 3.1 *(Continued)*

Affymetrix systemic name		Common name	Genbank ID	Description
1419664_at		*Srr*	BC011164	serine racemase
1419714_at		*Pdcd1lg1*	NM_021893	programmed cell death 1 ligand 1
1419967_at		*Seh1l*	AW540070	SEH1-like
1419970_at		*Slc35a5*	C86506	solute carrier family 35, member A5
1420034_at		*Ppp2r2d*	AU019644	protein phosphatase 2, regulatory subunit B, delta isoform (AU019644 Mouse eight-cell stage embryo cDNA *Mus musculus* cDNA clone J0520E06 3-, mRNA sequence)
1420052_x_at	*	*Psmb1*	C81484	proteasome (prosome, macropain) subunit, beta type 1
1420090_at	*	*Raf1*	AA990557	v-raf-1 leukemia viral oncogene 1
1420688_a_at		*Sgce*	NM_011360	sarcoglycan, epsilon
1420843_at	*	*Ptprf*	BF235516	protein tyrosine phosphatase, receptor type, F
1420872_at	*	*Gucy1b3*	BF472806	guanylate cyclase 1, soluble, beta 3
1421251_at		*Zfp40*	NM_009555	zinc finger protein 40
1421462_a_at		*Lepre1*	NM_019783	leprecan 1
1421619_at	*	*Kcnh3*	NM_010601	potassium voltage-gated channel, subfamily H (eag-related), member 3
1422025_at	*	*Mitf*	NM_008601	microphthalmia-associated transcription factor
1422218_at		*P2rx7*	NM_011027	purinergic receptor P2X, ligand-gated ion channel, 7
1423070_at		*Rpl21*	BG922742	general transcription factor III A
1423259_at		*Idb4*	BB121406	inhibitor of DNA binding 4
1423499_at		*Sncaip*	AK017012	synuclein, alpha interacting protein (synphilin)
1423677_at		*Fkbp9*	AF279263	FK506 binding protein 9
1424041_s_at		*C1s*	BC022123	complement component 1, s subcomponent
1424228_at		*Polr3h*	AK019868	polymerase (RNA) III (DNA directed) polypeptide H
1424295_at		*Dppa3*	AY082485	*Mus musculus* stella mRNA, complete cds
1424322_at		*Apex2*	AB072498	apurinic/apyrimidinic endonuclease 2

(Continued)

Table 3.1 *(Continued)*

Affymetrix systemic name		Common name	Genbank ID	Description
1424586_at		*Ehbp1*	AF424697	EH domain binding protein 1
1424651_at		*BC021611*	BC021611	hypothetical protein LOC257633
1424893_at		*Ndel1*	BC021434	nuclear distribution gene E-like homolog 1 (*A. nidulans*)
1425198_at		*Ptpn2*	BG076152	protein tyrosine phosphatase, non-receptor type 2
1425278_at		*Ube4a*	BC021406	ubiquitination factor E4A, UFD2 homolog (*S. cerevisiae*)
1425366_a_at		*Hus1*	AF076845	Hus1 homolog (*S. pombe*)
1425555_at	*	*Crk7/Crkrs*	BG070845	Cdc2-related kinase, arginine/serine-rich (RIKEN cDNA 1810022J16 gene)
1425597_a_at		*Qk*	AW060288	quaking
1425608_at		*Dusp3/VHR*	BC016269	dual specificity phosphatase 3 (vaccinia virus phosphatase VH1-related)
1425750_a_at		*Jak3*	L40172	Janus kinase 3
1425865_a_at		*Lig3*	U66057	ligase III, DNA, ATP-dependent
1425918_at		*Egln3*	BC022961	EGL nine homolog 3 (*C. elegans*)
1427558_s_at	*	*Alg12*	AJ429133	asparagine-linked glycosylation 12 homolog (yeast, alpha-1,6-mannosyltransferase)
1427595_at		*Acac*	BE650741	acetyl-Coenzyme A carboxylase alpha
1427833_at		*Spi16/mBM17*	U96702	serine protease inhibitor 16
1427843_at		*Cebpb*	AB012278	CCAAT/enhancer binding protein (C/EBP), beta
1428386_at		*Acsl3*	AK012088	acyl-CoA synthetase long-chain family member 3
1430148_at		*Rab19*	BM241400	RAB19, member RAS oncogene family
1430391_a_at		*Siat8d*	AK003690	sialyltransferase 8 (alpha-2,8-sialyltransferase) D
1430483_a_at		*Tmem79*	AK010144	transmembrane protein 79 (RIKEN cDNA 2310042N02 gene)
1430651_s_at		*Zfp191*	AI504586	zinc finger protein 191
1431066_at		*Fut11*	BB626220	fucosyltransferase 11

Table 3.1 *(Continued)*

Affymetrix systemic name		Common name	Genbank ID	Description
1432072_at	*	*Kif2a*	AK016720	kinesin family member 2A
1432115_a_at		*Pign*	AK014165	phosphatidylinositol glycan, class N
1433509_s_at		*Reep1*	BQ174328	receptor accessory protein 1(D6Ertd253e)
1433992_at	*	*Apxl*	BQ176992	apical protein, *Xenopus laevis*-like
1434349_at		*Vars2l*	AV258022	valyl-tRNA synthetase 2-like
1434369_a_at		*Cryab*	AV016515	crystallin, alpha B
1435132_at		*Disp1*	AI505698	dispatched homolog 1 (*Drosophila*)
1435557_at	*	*Fhod1*	AV298805	formin homology 2 domain containing 1
1435962_at		*Rps6*	BG089974	ribosomal protein S6 (Transcribed sequence with strong similarity to protein sp:P10660 (*H. sapiens*) RS6_HUMAN 40S ribosomal protein S6)
1436429_at		*Zfp606*	BB198855	zinc finger protein 606 (BB198855 RIKEN full-length enriched, 0 day neonate thymus *Mus musculus* cDNA clone A430007N09 3-, mRNA sequence)
1436521_at		*Slc36a2*	AI596194	solute carrier family 36 (proton/amino acid symporter), member 2
1436623_at		*Entpd7*	AV381133	ectonucleoside triphosphate diphosphohydrolase 7 (RIKEN cDNA 2900026G05 gene)
1436682_at		*Tmsb10*	AW259435	thymosin, beta 10 (up29e07.x1 NCI_CGAP_Mam2 *Mus musculus* cDNA clone IMAGE:2655780 3′ similar to gb:S54005 THYMOSIN BETA-10 (HUMAN), mRNA sequence)
1436895_at		*Centd1*	BB182934	centaurin, delta 1
1436904_at		*Thrap1*	BB667559	hypothetical protein D030023K18

(Continued)

Table 3.1 *(Continued)*

Affymetrix systemic name	Common name	Genbank ID	Description
1436993_x_at	*Pfn2*	BB560492	profilin 2 (BB560492 RIKEN full-length enriched, 10 days neonate olfactory brain *Mus musculus* cDNA clone E530111B09 3′ similar to AL096719 *Homo sapiens* mRNA; cDNA DKFZp566N043 (from clone DKFZp566N043), mRNA sequence.)
1437059_at	*Sox21*	BB046776	SRY-box containing gene 21 (BB046776 RIKEN full-length enriched, 11 days embryo *Mus musculus* cDNA clone 6230417M22 3-, mRNA sequence)
1437106_at	*Jarid1a*	BM246184	jumonji, AT rich interactive domain 1A (Rbp2 like) (K0734F05–3 NIA Mouse Hematopoietic Stem Cell (Lin-/c-Kit-/Sca-1-) cDNA Library (Long) *Mus musculus* cDNA clone NIA:K0734F05 IMAGE:30076864 3-, mRNA sequence)
1437123_at	*Mmrn2*	BB038352	multimerin 2
1437307_at	*Senp8*	BG069815	SUMO/sentrin specific protease family member 8
1437473_at	*Maf*	AV284857	avian musculoaponeurotic fibrosarcoma (v-maf) AS42 oncogene homolog (RIKEN cDNA A230108G15 gene)
1437789_at	*Birc6*	BB527646	baculoviral IAP repeat-containing 6 (BB527646 RIKEN full-length enriched, 15 days embryo head *Mus musculus* cDNA clone D930041P14 3-, mRNA sequence)
1437863_at	*Bche*	BB667762	butyrylcholinesterase (BB667762 RIKEN full-length enriched, adult male liver tumor *Mus musculus* cDNA clone C730038G20 3-, mRNA sequence)

Table 3.1 *(Continued)*

Affymetrix systemic name		Common name	Genbank ID	Description
1438463_x_at		*Zdhhc6*	AV142865	AV142865 *Mus musculus* C57BL/6J 10–11 day embryo *Mus musculus* cDNA clone 2810427C08, mRNA sequence.
1438825_at		*Calm3*	AV047570	calmodulin 3 (Similar to calmodulin – rabbit (tentative sequence) (LOC384465), mRNA (AV047570 *Mus musculus* adult C57BL/6J testis *Mus musculus* cDNA clone 1700069D17, mRNA sequence))
1438857_x_at		*Irak1*/pelle-like	BB058253	Irak1(interleukin-1 receptor-associated kinase 1)/pelle-like (BB058253 RIKEN full-length enriched, 2 days neonate sympathetic ganglion *Mus musculus* cDNA clone 7120478B17 3- similar to U56773 *Mus musculus*
1439247_at		*Dock10*	BB763030	dedicator of cytokinesis 10 (BB763030 RIKEN full-length enriched, B16 F10Y cells *Mus musculus* cDNA clone G370018M23 3-, mRNA sequence)
1440180_x_at		*Zbtb3*	AV258279	zinc finger and BTB domain containing 3 (AV258279 RIKEN full-length enriched, adult male testis (BNN132) *Mus musculus* cDNA clone 4923101A10 3', mRNA sequence)
1440871_at		*Baiap1*	AI835038	BAI1-associated protein 1
1441272_at	*	*Matr3*	BI249188	matrin 3 (602994742F1 NCI_CGAP_Mam5 *Mus musculus* cDNA clone IMAGE:5150530 5-, mRNA sequence)
1442100_at		*Inpp5f*	BB619843	inositol polyphosphate-5-phosphatase F

(Continued)

Table 3.1 *(Continued)*

Affymetrix systemic name		Common name	Genbank ID	Description
1443229_at		Atad2	AV319821	ATPase family, AAA domain containing 2 (RIKEN cDNA 2610509G12 gene (AV319821 RIKEN full-length enriched mouse cDNA library, C57BL/6J testis male 13 days embryo *Mus musculus* cDNA clone 6030413I17 3-, mRNA))
1443493_at		Dhx37	BB766805	DEAH (Asp–Glu–Ala–His) box polypeptide 37
1443952_at		Nr1d1	BI525006	nuclear receptor subfamily 1, group D, member 1 (602924093F1 NCI_CGAP_Lu33 *Mus musculus* cDNA clone IMAGE:5056607 5-, mRNA sequence)
1445195_at		C77631	C77631	expressed sequence C77631 (Mouse 3.5-dpc blastocyst cDNA *Mus musculus* cDNA clone J0035A08 3' similar to Mouse T-cell receptor (TCR V-alpha 16.1) gene exons 1–2, mRNA, mRNA sequence)
1447753_at		Cdc37l	BB391093	cell division cycle 37 homolog (*S. cerevisiae*)-like (BB391093 RIKEN full-length enriched, 0 day neonate cerebellum *Mus musculus* cDNA clone C230073C03 3-, mRNA sequence)
1447897_x_at		Anapc11	AV019615	AV019615 *Mus musculus* 18-day embryo C57BL/6J *Mus musculus* cDNA clone 1190010L24, mRNA sequence.
1448169_at		Krt1-18	NM_010664	keratin complex 1, acidic, gene 18
1448443_at		Serpini1	NM_009250	serine (or cysteine) proteinase inhibitor, clade I, member 1
1448986_x_at	*	Dnase2a	NM_010062	deoxyribonuclease II alpha

Table 3.1 *(Continued)*

Affymetrix systemic name		Common name	Genbank ID	Description
1449481_at		Slc25a13	BC016571	solute carrier family 25 (mitochondrial carrier; adenine nucleotide translocator), member 13
1449493_at		Insl5	NM_011831	insulin-like 5
1449700_at		Igbp1	C81413	immunoglobulin (CD79A) binding protein 1
1449789_x_at		Ly6g6c	AV088850	lymphocyte antigen 6 complex, locus G6C (*Mus musculus* tongue C57BL/6J adult *Mus musculus* cDNA clone 2310040E07, mRNA sequence)
1449851_at	*	Per1	AF022992	period homolog 1 (*Drosophila*)
1450046_at		Tmem59/ORF18	NM_019801	transmembrane protein 59 thymic dendritic cell-derived factor 1
1450135_at		Fzd3	AU043193	frizzled homolog 3 (*Drosophila*)
1450173_at		Ripk2	NM_138952	receptor (TNFRSF)-interacting serine-threonine kinase 2
1450199_a_at		Stab1	NM_138672	stabilin 1
1450208_a_at		Elmo1	NM_080288	engulfment and cell motility 1, ced-12 homolog (*C. elegans*)
1450296_at	*	Klrb1a	NM_010737	killer cell lectin-like receptor subfamily B member 1A
1450297_at		Il6	NM_031168	interleukin 6
1450424_a_at		Il18bp	AF110803	interleukin 18 binding protein
1451541_at		Bcs1l	BC019781	RIKEN cDNA 1700112N14 gene
1451583_a_at		BC025076	BC025076	hypothetical protein LOC216829 membrane magnesium transporter 2
1451592_at		P42pop	AF364868	Myb protein P42POP
1451768_a_at		Slc20a2	AF196476	solute carrier family 20, member 2
1451950_a_at		Cd80	D16220	CD80 antigen
1451996_at		Bbp	AF353993	beta-amyloid binding protein precursor
1452253_at		Crim1	AK018666	cysteine-rich motor neuron 1
1452905_at		Gtl2	AV015833	GTL2, imprinted maternally expressed untranslated mRNA

(Continued)

Table 3.1 *(Continued)*

Affymetrix systemic name		Common name	Genbank ID	Description
1453055_at		Sema6d	BB462688	sema domain, transmembrane domain (TM), and cytoplasmic domain, (semaphorin) 6D
1453227_at		Rhobtb3	BG801497	Rho-related BTB domain containing 3
1453481_at		Zdhhc2	BB342242	zinc finger, DHHC domain containing 2
1453690_at	*	Mpp7	AV292557	membrane protein, palmitoylated 7 (MAGUK p55 subfamily member 7) (RIKEN full-length enriched, 6 days neonate head *Mus musculus* cDNA clone 5430426E14 3′, mRNA sequence)
1454414_at	*	Btbd7	AK017755	BTB (POZ) domain containing 7
1455158_at		Itga3	BI664675	integrin alpha 3
1455297_at		SPIN-2	BG070258	Similar to Spindlin-like protein 2 (SPIN-2) (LOC278240), mRNA
1455404_at		Jph2	BG870711	junctophilin 2
1455717_s_at	*	Daam2	BM206030	dishevelled associated activator of morphogenesis 2
1455985_x_at		Shmt2	AV213251	serine hydroxymethyltransferase 2 (mitochondrial) (AV213251 RIKEN full-length enriched, ES cells *Mus musculus* cDNA clone 2410126G07 3′, mRNA sequence)
1456975_at		Taok1	BM238077	TAO kinase 1(RIKEN cDNA 2810468K05 gene)
1457040_at		Lgi2	BE947711	leucine-rich repeat LGI family, member 2
1457311_at		Camk2a	AW490258	calcium/calmodulin-dependent protein kinase II alpha
1457451_at		Acvr2	BB199213	activin receptor IIA
1458047_at		Tnfsf13b	BB667811	tumor necrosis factor (ligand) superfamily, member 13b
1458381_at		Clic5	BB028501	chloride intracellular channel 5
1458641_at		Braf	BM217816	Braf transforming gene

Table 3.1 *(Continued)*

Affymetrix systemic name	Common name	Genbank ID	Description
1459597_at	Mtpn	BG074849	myotrophin
1459868_x_at	Il11ra1	AV313111	interleukin 11 receptor, alpha chain 1 (RIKEN full-length enriched, adult male thymus *Mus musculus* cDNA clone 5830408C01 3′ similar to X74953 *M. musculus* ETL-2 mRNA, mRNA sequence.)
1460170_at	Ext2	NM_010163	exostoses (multiple) 2
1460666_a_at	Ebf3	NM_010096	early B-cell factor 3

*: overlapped in both lists of union genes for radiation-induced and spontaneous leukemias.

10 genes that represent the 128 genes mentioned above are described as follows: *Eef1a2* (eukaryotic translation elongation factor 1 alpha 2), expressed in tumors of the ovary, breast and lung (Amiri *et al.*, 2007; Tomlinson *et al.*, 2007) and plays a role in the resistance to apoptosis induced by oxidative stress (Chang and Wang, 2007); *Top3a* (topoisomerase (DNA) III alpha), required for accurate DNA replication (Oh *et al.*, 2002) and related to telomere–telomere recombination (Tsai *et al.*, 2006), cancer, and aging (Laursen *et al.*, 2003); *Ppp2r2d* (protein phosphatase 2, regulatory subunit B, delta isoform), expression biomarker for blast crisis (Liu *et al.*, 2007; Neviani *et al.*, 2007); *Lepre1* (leprecan 1), basement-membrane-associated proteoglycan that functions in growth suppression and is a potential suppressor gene (Wassenhove-McCarthy and McCarthy, 1999); *Idb4* (inhibitor of DNA binding4), promotes neuronal stem cell proliferation (Yun *et al.*, 2004) and induction of leukemia cell apoptosis (Yu *et al.*, 2005); *Hus1* (hydroxyurea sensitive1), DNA damage checkpoint (Harris *et al.*, 2006), required for telomere maintenance and functions as Rad9–Hus1–Rad1 checkpoint; *Dusp3/VHR* (dual-specificity phosphatase 3 (vaccinia virus phosphatase VH1-related)), induces expression of cyclin D1 in breast cancer (Hao *et al.*, 2007) and arrests the cell cycle in VHR (Rahmouni *et al.*, 2006); *Igbp1/alpha 4* (immunoglobulin (CD79A) binding protein 1), apoptosis inhibitor via dephosphorylation of c-Jun and p53 (Kong *et al.*, 2004) and biomarker for acute myelogenous leukemia (Cruse *et al.*, 2005; Bhargava *et al.*, 2007); *Itga3* (integrin alpha 3), inhibitor of caspase 3 activity (Manohar *et al.*, 2004), which is up-regulated in adenocarcinoma of the lung (Boelens *et al.*, 2007), esophagus (Hourihan *et al.*, 2003) and stomach (Varis *et al.*, 2002); *Il11ra1* (Interleukin 11 receptor alpha 1), functions in carcinogenesis associated with up-regulation of PI3K and p44/p42 MAPK in gastric cancer (Nakayama *et al.*, 2007) and colon cancer (Yoshizaki *et al.*, 2006) associated with STAT3 in the prostate cancer (Zurita *et al.*, 2004), and constitutively activated in myeloma/B-CLL (Tsimanis *et al.*, 2001). The functions of these genes may satisfy the characteristics of cluster-specific gene expression profiles linked to radiation-induced leukemias.

Among the 149 genes, 21 genes, including *raf1*, *Mitf*, and *Crkrs*, overlap in both lists of union genes for both radiation-induced and spontaneous leukemias (see asterisks in

Table 3.1). These overlapped genes observed in both union gene lists imply that not all the radiation-specific union genes (i.e. 'stochastically necessary genes') are always required for the development of radiation-induced myelogenous leukemias, but a combination of the 'stochastically necessary genes' in the list is required in addition to the common leukemogenic genes. An essential rule for the combination of the 'stochastically necessary genes' for radiation-induced leukemogenicity is not yet identified.

3.9 New Risk Evaluation Strategy Using Gene Expression Profiles

These toxicological endpoints obtained by gene chip and microarray technologies can be used to evaluate their quantitative and qualitative differences in gene expression for risk evaluation by PCA. Figure 3.9a shows sample expression data between the two groups, one for bone marrow tissues exposed to 0.6 Gy and the other for nonirradiated controls, which is shown by two-dimensional expressions from PCA components #1 and #2. No observed effect level (NOEL) or no observed adverse effect level (NOAEL) can be statistically calculated by the 95 % confidence areas of the two clusters, so that the differences between the two groups can be considered as the risk evaluation parameters. Furthermore, when one attempts to evaluate the possible differences between the two groups by gene chip and microarray methods, one can use any component(s) with low differential contribution. However, when one attempts to evaluate homogeneity, one should evaluate possible

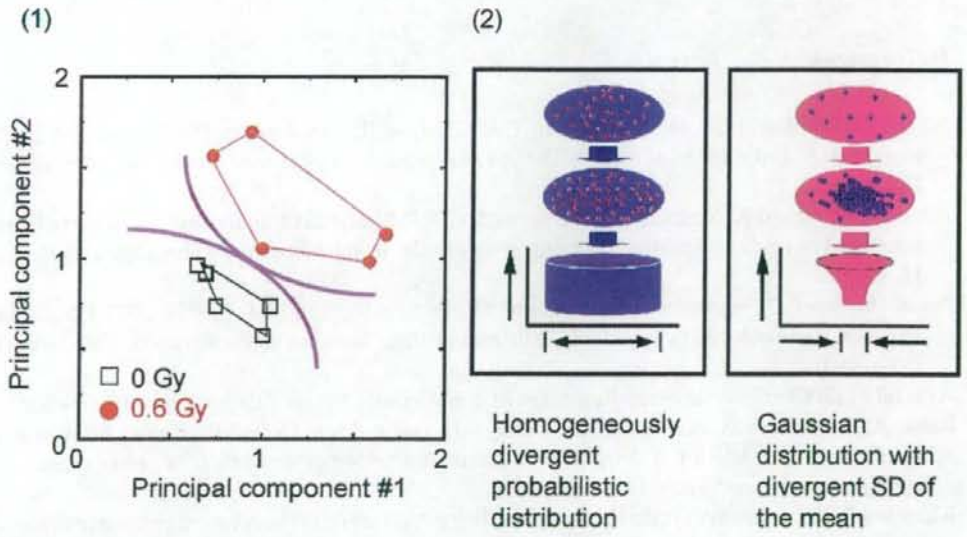

Figure 3.9 *(a) Sample gene expression clusters associated with the bone marrow after 0.6 Gy whole-body irradiation and those associated with the control are shown in the two-dimensional principal component diagram plotted along the contribution factors. Areas of each cluster are statistically defined along with the confidence levels of NOEL and/or NOAEL. See text. (b) Two types of data distribution pattern: homogeneously divergent probabilistic distribution on the left and divergent distribution due to Gaussian distribution with the error of the mean on the right.*

consistencies not only for the major component, but also for other components with low contribution, and determine whether the differences can be ignored. Because minor components may sometimes play an important toxicological role, careful examination of the genomic repertoire is required to determine whether the expressions of responsible genes are identical in a case-by-case manner.

Lastly, it is very important to recognize the characteristics of each data point. When one calculates NOEL or NOAEL, one should note the different characteristics and diversity of data between the two types, such as whether the data show probabilistic homogeneously diverse distribution or a Gaussian normal equivalent distribution due to error/deviation, as shown on the left and right sides of Figure 3.9b. Interestingly, data from developmental toxicology and the growth parameters tend to show the latter convergent distribution. However, data from toxicological changes in relation to senescence tend to show the former scattered distribution.

In this chapter, murine spontaneous and radiation-induced myelogenous leukemias were used as experimental models to discuss an essential principle of data-mining in toxicogenomics. The examinations were focused only on the bone marrow. A possible reason for the predictability observed in tissues other than the bone marrow may be attributable to the characteristics of radiation-induced tissue injury, of which the general rule may be stochastic but generally applicable to other tissues. In the case of chemicals, the predictability of the results of a single tissue examination may be limited owing to the possible tissue-specific interactions of such test chemicals.

References

Adams MD, Celniker SE, Holt RA, Evans CA, Gocayne JD, Amanatides PG, Scherer SE, Li PW, Hoskins RA, Galle RF *et al.* (2000) The genome sequence of *Drosophila melanogaster*. *Science* **287**, 2185–2195.

Albanese J, Martens K, Karkanitsa LV, Dainiak N (2007) Multivariate analysis of low-dose radiation-associated changes in cytokine gene expression profiles using microarray technology. *Exp Hematol* **35**, 47–54.

Amiri A, Noei F, Jeganathan S, Kulkarni G, Pinke DE, Lee JM (2007) eEF1A2 activates Akt and stimulates Akt-dependent actin remodeling, invasion and migration. *Oncogene* **26**, 3027–3040.

Astrand M (2003) Contrast normalization of oligonucleotide arrays. *J Comput Biol* **10**, 95–102.

Bahar R, Hartmann CH, Rodriguez KA, Denny AD, Busuttil RA, Dolle ME, Calder RB, Chisholm GB, Pollock BH, Klein CA, Vijg J (2006) Increased cell-to-cell variation in gene expression in ageing mouse heart. *Nature* **441**, 1011–1014.

Bhargava P, Kallakury BV, Ross JS, Azumi N, Bagg A (2007) CD79a is heterogeneously expressed in neoplastic and normal myeloid precursors and megakaryocytes in an antibody clone-dependent manner. *Am J Clin Pathol* **128**, 306–313.

Bloomfield VA, Crothers DM, Tinoco I (2000) Nucleic Acids: Structures, Properties, and Functions. University Science Books: Sausalito, CA.

Boelens MC, van den Berg A, Vogelzang I, Wesseling J, Postma DS, Timens W, Groen HJ (2007) Differential expression and distribution of epithelial adhesion molecules in non-small cell lung cancer and normal bronchus. *J Clin Pathol* **60**, 608–614.

Borlak J (2005) *Handbook of Toxicogenomics*. Wiley–VCH Verlag: Weinheim.

Brazma A, Hingamp P, Quackenbush J, Sherlock G, Spellman P, Stoeckert C, Aach J, Ansorge W, Ball CA, Causton HC *et al.* (2001) Minimum information about a microarray experiment (MIAME) – toward standards for microarray data. *Nat Genet* **29**, 365–371.

Brenner S, Jacob F, Meselson M (1961) An unstable intermediate carrying information from genes to ribosomes for protein synthesis. *Nature* **190**, 576–581.

Brown PO, Botstein D (1999) Exploring the new world of the genome with DNA microarrays. *Nat Genet* **21**, 33–37.

C. elegans Sequencing Consortium (1998) Genome sequence of the nematode *C. elegans*: a platform for investigating biology. *Science* **282**, 2012–2018.

Chang R, Wang E (2007) Mouse translation elongation factor eEF1A-2 interacts with Prdx-I to protect cells against apoptotic death induced by oxidative stress. *J Cell Biochem* **100**, 267–278.

Churchill GA (2002) Fundamentals of experimental design for cDNA microarrays. *Nat Genet* **32** (Suppl.), 490–495.

Crick FH (1958) On protein synthesis. *Symp Soc Exp Biol* **12**, 138–163.

Crick FH, Barnett L, Brenner S, Watts-Tobin RJ (1961) General nature of the genetic code for proteins. *Nature* **192**, 1227–1232.

Cruse JM, Lewis RE, Pierce S, Lam J, Tadros Y (2005) Aberrant expression of CD7, CD56, and CD79a antigens in acute myeloid leukemias. *Exp Mol Pathol* **79**, 39–41.

Czapski G, Peled E (1973) Reaction rates of electrons at short times. *J Phys Chem* **77**, 893.

Czapski G, Peled E (1975) Reaction rates of electrons at short times. In *Radiation Research: Biomedical, Chemical and Physical Perspectives*, OF Nygaard, HI Adler, WK Sinclair (eds). Academic Press: New York.

Fodor SP, Rava RP, Huang XC, Pease AC, Holmes CP, Adams CL (1993) Multiplexed biochemical assays with biological chips. *Nature* **364**, 555–556.

Hamadeh HK, Bushel P, Paules R, Afshari CA (2001) Discovery in toxicology: mediation by gene expression array technology. *J Biochem Mol Toxicol* **15**, 231–242.

Hao L, El Shamy WM (2007) BRCA1-IRIS activates cyclin D1 expression in breast cancer cells by downregulating the JNK phosphatase DUSP3/VHR. *Int J Cancer* **121**, 39–46.

Harris J, Lowden M, Clejan I, Tzoneva M, Thomas JH, Hodgkin J, Ahmed S (2006) Mutator phenotype of *Caenorhabditis elegans* DNA damage checkpoint mutants. *Genetics* **174**, 601–616.

Hastie ND, Allshire RC (1989) Human telomeres: fusion and interstitial sites. *Trends Genet* **5**, 326–331.

Henke FU, Lubarsch O (1924–1952). *Handbuch des speziellen pathologischen Anatomie und Histologie*, vols **1–12**. Springer: Berlin.

Hill AA, Brown EL, Whitley MZ, Tucker-Kellogg G, Hunter CP, Slonim DK (2001) Evaluation of normalization procedures for oligonucleotide array data based on spiked cRNA controls. *Genome Biol* **2**, RESEARCH0055.

Hourihan RN, O'Sullivan GC, Morgan JG (2003) Transcriptional gene expression profiles of oesophageal adenocarcinoma and normal oesophageal tissues. *Anticancer Res* **23**, 161–165.

Hu T, Gibson DP, Carr GJ, Torontali SM, Tiesman JP, Chaney JG, Aardema MJ (2004) Identification of a gene expression profile that discriminates indirect-acting genotoxins from direct-acting genotoxins. *Mutat Res* **549**, 5–27.

Hunt JW (1976) Early events in radiation chemistry. In *Advances in Radiation Chemistry*, vol. **5**, M Burton, JL Magee (eds). John Wiley and Sons, Ltd: New York, p. 185.

Inoue T (2003) Introduction: Toxicogenomics – a New Paradigm of Toxocology. In *Toxicogenomics*, T Inoue, WD Pennie (eds). Springer-Verlag: Tokyo, pp. 3–11.

Kong M, Fox CJ, Mu J, Solt L, Xu A, Cinalli RM, Birnbaum MJ, Lindsten T, Thompson CB (2004) The PP2A-associated protein alpha4 is an essential inhibitor of apoptosis. *Science* **306**, 695–698.

Kroll TC, Wolfl S (2002) Ranking: a closer look on globalisation methods for normalisation of gene expression arrays. *Nucleic Acids Res* **30**, e50.

Lander ES, Linton LM, Birren B, Nusbaum C, Zody MC, Baldwin J, Devon K, Dewar K, Doyle M, FitzHugh W *et al.* (2001) Initial sequencing and analysis of the human genome. *Nature* **409**, 860–921.

Laursen LV, Bjergbaek L, Murray JM, Andersen AH (2003) RecQ helicases and topoisomerase III in cancer and aging. *Biogerontology* **4**, 275–87.

Lewin, B (2004) *Genes VIII*. Pearson Prentice Hall, Upper Saddle River, NJ.

Liu Q, Zhao X, Frissora F, Ma Y, Santhanam R, Jarjoura D, Lehman A, Perrotti D, Chen CS, Dalton JT, Muthusamy N, Byrd JC (2007) FTY720 demonstrates promising pre-clinical activity for chronic lymphocytic leukemia and lymphoblastic leukemia/lymphoma. *Blood* **111**, 275–284.

Lodish H, Berk A, Matsudaira P, Kaiser C, Krieger M, Scott M, Zipursky SL, Darnell J (2004) *Molecular Cell Biology*. WH Freeman: New York.

Lovett RA (2000) Toxicogenomics. Toxicologists brace for genomics revolution. *Science* **289**, 536–537.

Manohar A, Shome SG, Lamar J, Stirling L, Iyer V, Pumiglia K, DiPersio CM (2004) Alpha 3 beta 1 integrin promotes keratinocyte cell survival through activation of a MEK/ERK signaling pathway. *J Cell Sci* **117**, 4043–4054.

Nakayama T, Yoshizaki A, Izumida S, Suehiro T, Miura S, Uemura T, Yakata Y, Shichijo K, Yamashita S, Sekin I (2007) Expression of interleukin-11 (IL-11) and IL-11 receptor alpha in human gastric carcinoma and IL-11 upregulates the invasive activity of human gastric carcinoma cells. *Int J Oncol* **30**, 825–833.

Neviani P, Santhanam R, Oaks JJ, Eiring AM, Notari M, Blaser BW, Liu S, Trotta R, Muthusamy N, Gambacorti-Passerini C, Druker BJ, Cortes J, Marcucci G, Chen CS, Verrills NM, Roy DC, Caligiuri MA, Bloomfield CD, Byrd JC, Perrotti D (2007) FTY720, a new alternative for treating blast crisis chronic myelogenous leukemia and Philadelphia chromosome-positive acute lymphocytic leukemia. *J Clin Invest* **117**, 2408–2421.

Oh M, Choi IS, Park SD (2002) Topoisomerase III is required for accurate DNA replication and chromosome segregation in *Schizosaccharomyces pombe*. *Nucleic Acids Res* **30**, 4022–4031.

Petersen D, Chandramouli GV, Geoghegan J, Hilburn J, Paarlberg J, Kim CH, Munroe D, Gangi L, Han J, Puri R, Staudt L, Weinstein J, Barrett JC, Green J, Kawasaki ES (2005) Three microarray platforms: an analysis of their concordance in profiling gene expression. *BMC Genomics* **6**, 63.

Rahmouni S, Cerignoli F, Alonso A, Tsutji T, Henkens R, Zhu C, Louis-dit-Sully C, Moutschen M, Jiang W, Mustelin T (2006) Loss of the VHR dual-specific phosphatase causes cell-cycle arrest and senescence. *Nat Cell Biol* **8**, 524–531.

Schadt EE, Li C, Ellis B, Wong WH (2001) Feature extraction and normalization algorithms for high-density oligonucleotide gene expression array data. *J Cell Biochem Suppl* **37**, 120–125.

Seki M, Yoshida K, Nishimura M, Nemoto K (1991) Radiation-induced myeloid leukemia in C3H/He mice and the effect of prednisolone acetate on leukemogenesis. *Radiat Res* **127**, 146–149.

Singer M, Berg P (1991) *Genes & Genomes: A Changing Perspective*. University Science Books: Mill Valley, CA.

Storck T, von Brevern MC, Behrens CK, Scheel J, Bach A (2002) Transcriptomics in predictive toxicology. *Curr Opin Drug Discov Dev* **5**, 90–97.

Stoyanova R, Querec TD, Brown TR, Patriotis C (2004) Normalization of single-channel DNA array data by principal component analysis. *Bioinformatics* **20**, 1772–1784.

Tomlinson VA, Newbery HJ, Bergmann JH, Boyd J, Scott D, Wray NR, Sellar GC, Gabra H, Graham A, Williams AR, Abbott CM (2007) Expression of eEF1A2 is associated with clear cell histology in ovarian carcinomas: overexpression of the gene is not dependent on modifications at the EEF1A2 locus. *Br J Cancer* **96**, 1613–1620.

Tsai HJ, Huang WH, Li TK, Tsai YL, Wu KJ, Tseng SF, Teng SC (2006) Involvement of topoisomerase III in telomere–telomere recombination. *J Biol Chem* **281**, 13717–13723.

Tsimanis A, Shvidel L, Klepfish A, Shtalrid M, Kalinkovich A, Berrebi A (2001) Over-expression of the functional interleukin-11 alpha receptor in the development of B-cell chronic lymphocytic leukemia. *Leuk Lymphoma* **42**, 195–205.

Varis A, Wolf M, Monni O, Vakkari ML, Kokkola A, Moskaluk C, Frierson Jr H, Powell SM, Knuutila S, Kallioniemi A, El-Rifai W (2002) Targets of gene amplification and overexpression at 17q in gastric cancer. *Cancer Res* **62**, 2625–2629.

Wassenhove-McCarthy DJ, McCarthy KJ (1999) Molecular characterization of a novel basement membrane-associated proteoglycan, leprecan. *J Biol Chem* **274**, 25004–25017.

Waterston RH, Lindblad-Toh K, Birney E, Rogers J, Abril JF, Agarwal P, Agarwala R, Ainscough R, Alexandersson M, An P *et al.* (2002) Initial sequencing and comparative analysis of the mouse genome. *Nature* **420**, 520–562.

Watson JD, Baker TA, Bell SP, Gann A, Levine M, Losick T (2007) *Molecular Biology of the Gene.* Pearson/Benjamin Cummings: San Francisco, CA.

Watson JD, Crick FH (1953) Molecular structure of nucleic acids; a structure for deoxyribose nucleic acid. *Nature* **171**, 737–738.

Yoshida K, Inoue T, Nojima K, Hirabayashi Y, Sado T (1997) Calorie restriction reduces the incidence of myeloid leukemia induced by a single whole-body radiation in C3H/He mice. *Proc Natl Acad Sci U S A* **94**, 2615–2619.

Yoshizaki A, Nakayama T, Yamazumi K, Yakata Y, Taba M, Sekine I (2006). Expression of interleukin (IL)-11 and IL-11 receptor in human colorectal adenocarcinoma: IL-11 up-regulation of the invasive and proliferative activity of human colorectal carcinoma cells. *Int J Oncol* **29**, 869–876.

Yu L, Liu C, Vandeusen J, Becknell B, Dai Z, Wu YZ, Raval A, Liu TH, Ding W, Mao C, Liu S, Smith LT, Lee S, Rassenti L, Marcucci G, Byrd J, Caligiuri MA, Plass C (2005) Global assessment of promoter methylation in a mouse model of cancer identifies ID4 as a putative tumor-suppressor gene in human leukemia. *Nat Genet* **37**, 265–274.

Yun K, Mantani A, Garel S, Rubenstein J, Israel MA (2004) Id4 regulates neural progenitor proliferation and differentiation *in vivo*. *Development* **131**, 5441–5448.

Yunis JJ, Soreng AL, Bowe AE (1987) Fragile sites are targets of diverse mutagens and carcinogens. *Oncogene* **1**, 59–69.

Zhang W, Shmulevich I (2006) *Computational and Statistical Approaches to Genomics*. Springer Science+Business Media: New York.

Zurita AJ, Troncoso P, Cardo-Vila M, Logothetis CJ, Pasqualini R, Arap W (2004) Combinatorial screenings in patients: the interleukin-11 receptor alpha as a candidate target in the progression of human prostate cancer. *Cancer Res* **64**, 435–439.

Neuroscience 155 (2008) 780–788

IDENTIFICATION OF GENES THAT RESTRICT ASTROCYTE DIFFERENTIATION OF MIDGESTATIONAL NEURAL PRECURSOR CELLS

T. SANOSAKA,[a] M. NAMIHIRA,[a] H. ASANO,[a] J. KOHYAMA,[a] K. AISAKI,[b] K. IGARASHI,[b] J. KANNO[b] AND K. NAKASHIMA[a]*

[a]*Laboratory of Molecular Neuroscience, Graduate School of Biological Sciences, Nara Institute of Science and Technology, 8916-5, Takayama, Ikoma, Nara 630-0101, Japan*

[b]*Division of Cellular and Molecular Toxicology, Biological Safety Research Center, National Institutes of Health Sciences, 1-18-1, Kamiyoga, Setagaya-ku, Tokyo 158-8501, Japan*

Abstract—During development of the mammalian CNS, neurons and glial cells (astrocytes and oligodendrocytes) are generated from common neural precursor cells (NPCs). However, neurogenesis precedes gliogenesis, which normally commences at later stages of fetal telencephalic development. Astrocyte differentiation of mouse NPCs at embryonic day (E) 14.5 (relatively late gestation) is induced by activation of the transcription factor signal transducer and activator of transcription (STAT) 3, whereas at E11.5 (mid-gestation) NPCs do not differentiate into astrocytes even when stimulated by STAT3-activating cytokines such as leukemia inhibitory factor (LIF). This can be explained in part by the fact that astrocyte-specific gene promoters are highly methylated in NPCs at E11.5, but other mechanisms are also likely to play a role. We therefore sought to identify genes involved in the inhibition of astrocyte differentiation of NPCs at midgestation. We first examined gene expression profiles in E11.5 and E14.5 NPCs, using Affymetrix GeneChip analysis, applying the Percellome method to normalize gene expression level. We then conducted *in situ* hybridization analysis for selected genes found to be highly expressed in NPCs at midgestation. Among these genes, we found that *N-myc* and high mobility group AT-hook 2 (*Hmga2*) were highly expressed in the E11.5 but not the E14.5 ventricular zone of mouse brain, where NPCs reside. Transduction of *N-myc* and *Hmga2* by retroviruses into E14.5 NPCs, which normally differentiate into astrocytes in response to LIF, resulted in suppression of astrocyte differentiation. However, sustained expression of *N-myc* and *Hmga2* in E11.5 NPCs failed to maintain the hypermethylated status of an astrocyte-specific gene promoter. Taken together, our data suggest that astrocyte differentiation of NPCs is regulated not only by DNA methylation but also by genes whose expression is controlled spatio-temporally during brain development.

*Corresponding author. Tel: +81-743-72-5471; fax: +81-743-72-5479.
E-mail address: kin@bs.naist.jp (K. Nakashima).

Abbreviations: bHLH, basic helix–loop–helix; BMP, bone morphogenetic protein; CNTF, ciliary neurotrophic factor; CT-1, cardiotrophin-1; DIG, digoxigenin; E, embryonic day; Gapdh, glyceraldehyde-3-phosphate dehydrogenase; GEO, Gene Expression Omnibus; *gfap*, glial fibrillary acidic protein; *Hmga2*, high mobility group AT-hook 2; JAK, janus kinase; LIF, leukemia inhibitory factor; NPC, neural precursor cell; SSC, sodium chloride sodium citrate; STAT, signal transducer and activator of transcription.

0306-4522/08$32.00+0.00 © 2008 IBRO. Published by Elsevier Ltd. All rights reserved.
doi:10.1016/j.neuroscience.2008.06.039

Key words: *N-myc*, *Hmga2*, epigenetics, Percellome method, differentiation.

The mammalian CNS is composed of neurons, astrocytes, and oligodendrocytes. Although these three cell types are derived from common multipotent neural precursor cells (NPCs), their differentiation is spatially and temporally regulated during development (Temple, 2001). Fetal telencephalic NPCs divide symmetrically in early gestation to increase their own numbers, and then undergo neurogenesis through mostly asymmetric divisions. Toward the end of the neurogenic phase, NPCs acquire multipotentiality to generate astrocytes and oligodendrocytes as well as neurons. It has recently become apparent that NPC fate determination is controlled by both extracellular cues, including cytokine signaling, and intracellular programs such as epigenetic gene regulation (Edlund and Jessell, 1999; Takizawa et al., 2001; Hsieh and Gage, 2004).

Interleukin (IL) -6 family cytokines such as cardiotrophin-1 (CT-1), leukemia inhibitory factor (LIF) and ciliary neurotrophic factor (CNTF) activate the janus kinase (JAK) –signal transducer and activator of transcription (STAT) signaling pathway and are known to induce astrocyte differentiation of NPCs (Bonni et al., 1997; Rajan and McKay, 1998). Gene knockouts of LIF (Bugga et al., 1998), LIF receptor β (Koblar et al., 1998), the common receptor component gp130 (Nakashima et al., 1999a) and STAT3 (He et al., 2005) all result in impaired astrocyte differentiation *in vivo*, emphasizing the contribution of JAK-STAT signaling to astrogliogenesis in the developing CNS. Bone morphogenetic proteins (BMPs) are another group of astrocyte-inducing cytokines. They synergistically induce astrocytic differentiation of NPCs via formation of a complex between STATs and BMP-activated transcription factor Smads, bridged by the transcriptional coactivators p300/CBP (Nakashima et al., 1999b).

In addition to these extracellular factors, intracellular programs and factors also play critical roles to regulate astrocytic differentiation of NPCs. We have previously shown that a CpG dinucleotide within a STAT3-binding element (TTC*CG*AGAA) in the astrocytic marker glial fibrillary acidic protein (*gfap*) gene promoter is highly methylated in NPCs at midgestation (embryonic day (E)11.5), when the cells differentiate only into neurons but not into astrocytes. Since STAT3 does not bind to the methylated cognate sequence, NPCs at midgestation do not express *gfap* even when stimulated by STAT3-activating cytokines such as LIF. As gestation proceeds, the STAT3-binding

site becomes gradually demethylated in NPCs, enabling them to express *gfap* in response to LIF stimulation (Takizawa et al., 2001). Thus, we have proposed that DNA methylation is a critical cell-intrinsic determinant of astrocyte differentiation during brain development. However, the important question of how this astrocyte-specific gene promoter becomes demethylated in NPCs remains unanswered.

Neurogenic basic helix–loop–helix (bHLH) transcription factors have been also shown to regulate astrocyte differentiation during early neural development. Mice carrying mutations in *mash1* and *math3* (Tomita et al., 2000), or, to a lesser extent, *mash1* and *ngn2* (Nieto et al., 2001) exhibit decreased neurogenesis and premature astrogliogenesis. Conversely, overexpression of neurogenic bHLH factors, either *in vivo* during the gliogenic period (Cai et al., 2000) or in cultured NPCs exposed to CNTF (Sun et al., 2001), promotes neurogenesis at the expense of astrogliogenesis. A possible mechanism underlying the repressive effect on astrogliogenesis is that Ngn1 binds to p300/CBP and sequesters them away from STAT3, thereby preventing STAT3 from activating astrocytic gene expression (Sun et al., 2001). Such a mechanism may ensure the restriction of astrocyte differentiation in NPCs that would otherwise differentiate into neurons under the influence of high-level neurogenic bHLH factor expression during the neurogenic period.

Although these studies have provided us with an integrated insight into the mechanism of neurogenic-to-gliogenic switching in NPCs, they do not preclude the involvement of other, as yet unknown, factors. To identify such factors, we first in this study examined gene expression profiles of mid- and late-gestational NPCs by Affymetrix GeneChip analysis, which is widely used to obtain a complete picture of developmental stage-specific gene expression (Abramova et al., 2005; Ajioka et al., 2006). We then performed *in situ* hybridization experiments to investigate the spatio-temporal expression pattern of genes that were found to be highly expressed in midgestational NPCs. Two genes, *N-myc* and high mobility group AT-hook 2 (*Hmga2*), were highly expressed in the ventricular zone of E11.5 but not of E14.5 mouse brain. Transduction of *N-myc* and *Hmga2* into E14.5 NPCs resulted in suppression of astrocyte differentiation, even in the presence of LIF. However, the prolonged expression of these genes in E11.5 NPCs failed to preserve the hypermethylated status of the astrocyte-specific *gfap* promoter. These results suggest that the inhibition of astrocyte differentiation in midgestational NPCs is regulated not only by DNA methylation of astrocyte-specific gene promoters but also by transcription-regulating factors whose expression is controlled spatio-temporally during brain development.

EXPERIMENTAL PROCEDURES

NPC culture

Timed-pregnant ICR mice were used to prepare NPCs. The protocols described below were carried out according to the animal experimentation guidelines of Nara Instititute of Science and Technology that comply with National Institutes of Health Guide for Care and Use of Laboratory Animals. All efforts were made to minimize the number of animals used and their suffering. NPCs were prepared from telencephalons of E11.5 and E14.5 mice and cultured as described previously (Nakashima et al., 1999b). Briefly, the telencephalons were triturated in Hanks' balanced salt solution by mild pipetting with a 1-ml pipet tip (Gilson, Middleton, WI, USA). Dissociated cells were cultured in N2-supplemented Dulbecco's Modified Eagle's Medium with F12 (GIBCO, Grand Island, NY, USA) containing 10 ng/ml basic FGF (R&D Systems, Minneapolis, MN, USA) (N2/DMEM/F12/bFGF) on culture dishes (Nunc, Naperville, IL, USA) or chamber slides (Nunc) which had been precoated with poly-L-ornithine (Sigma, St. Louis, MO, USA) and fibronectin (Sigma).

Immunocytochemistry

E11.5 and E14.5 NPCs cultured on coated chamber slides were washed with PBS, fixed in 4% paraformaldehyde in PBS, and stained with the following primary antibodies: rabbit anti-SOX2 (1:1000, Chemicon, Temecula, CA, USA), mouse anti-βIII-tubulin (1:500, Sigma), rabbit anti-GFAP (1:2000, Dako, High Wycombe, UK). The following secondary antibodies were used: Alexa488-conjugated goat anti-rabbit IgG (1:500, Molecular Probes, Eugene, OR, USA), Cy3-conjugated goat anti-mouse IgG (1:500, Chemicon). Nuclei were stained using bisbenzimide H33258 fluorochrome trihydrochloride (Nacalai Tesque, Kyoto, Japan). All experiments were independently replicated at least three times.

Sample preparation and GeneChip analysis

These procedures were conducted according to the Percellome method (Kanno et al., 2006) to normalize mRNA expression values to sample cell numbers by adding external spike mRNAs to the sample in proportion to the genomic DNA concentration and utilizing the spike RNA quantity data as a dose-response standard curve for each sample. Cells cultured on coated dishes were washed with PBS, lysed in 500 ml of RLT buffer (Qiagen K.K., Tokyo, Japan) and transferred to a 1.5-ml tube. Two separate 10-μl aliquots were treated with DNAse-free RNase A (Nippon Gene, Tokyo, Japan) for 30 min at 37 °C, followed by proteinase K (Roche Diagnostics, Mannheim, Germany) for 3 h at 55 °C, and then transferred to a 96-well black plate. PicoGreen fluorescent dye (Molecular Probes) was added to each well, and then incubated for 2 min at 30 °C. The DNA concentration was measured using a 96-well fluorescence plate reader with excitation at 485 nm and emission at 538 nm. Lamda phage DNA (PicoGreen kit, Molecular Probes) was used as standard. The appropriate amount of spike RNA cocktail was added to the sample homogenates in proportion to their DNA concentration. Five independent *Bacillus subtilis* poly-A RNAs were included in the grade-dosed spike cocktail. Total RNAs were purified using an RNeasy Mini kit (Qiagen), according to the manufacturer's instructions. First-strand cDNAs were synthesized by incubating 5 μg of total RNA with 200 U SuperScript II reverse transcriptase (Invitrogen, Carlsbad, CA, USA) and 100 pmol T7-$(dT)_{24}$ primer [5′-GGCCAGTGAATTGTAATACGACTCACTATAGGGAGGCGG-$(dT)_{24}$-3′]. After second-strand synthesis, the double-stranded cDNAs were purified using a GeneChip Sample Cleanup Module (Affymetrix, Washington, DC, USA), according to the manufacturer's instructions, and labeled by *in vitro* transcription using a BioArray HighYield RNA transcript labeling kit (Enzo Life Sciences, Farmingdale, NY, USA). The labeled cRNA was then purified using a GeneChip Sample Cleanup Module (Affymetrix) and treated with fragmentation buffer at 94 °C for 35 min. For hybridization to a GeneChip Mouse Genome 430 2.0 Array (Affymetrix), 15 μg of fragmented cRNA probe was incubated with 50 pM control oligonucleotide B2, 1× eukaryotic hybridization control (1.5 pM BioB, 5 pM BioC, 25 pM BioD and 100 pM Cre), 0.1 mg/ml herring sperm

DNA, 0.5 mg/ml acetylated BSA and 1× manufacturer-recommended hybridization buffer in a 45 °C rotisserie oven for 16 h. Washing and staining were performed in a GeneChip Fluidics Station (Affymetrix) using the appropriate antibody amplification, washing and staining protocols. The phycoerythrin-stained arrays were scanned as digital image files, which were analyzed with GeneChip Operating Software (Affymetrix). The expression data were converted to copy numbers of mRNA per cell by the Percellome method, quality controlled, and analyzed using Percellome software (Kanno et al., 2006). The GeneChip data have been deposited in the NCBI Gene Expression Omnibus (GEO; http://www.ncbi.nlm.nih.gov/geo/) and is accessible through GEO series accession number GSE 10796.

Quantitative real-time RT-PCR

Quantitative real-time PCR was performed to confirm the results of GeneChip analysis. RNAs from E11.5 and E14.5 NPCs were reverse transcribed using Superscript II (Invitrogen) and amplified by PCR, with a specific pair of primers for each gene, using the Mx3000P system (Stratagene, La Jolla, CA, USA). The expression of target genes was normalized to that of glyceraldehyde-3-phosphate dehydrogenase (*Gapdh*). The gene-specific primers were as follows: mouse N-myc: N-myc-S, 5′-aactatgctgcaccctcacc-3′; N-myc-AS, 5′-tagcaagtccgagcgtgttc-3′; mouse Hmga2: Hmga2-S, 5′-ggcagccgtccacatcag-3′; Hmga2-AS, 5′-taatcctcctctgcggactc-3′; mouse Sox11: Sox11-S, 5′-gagcctgtacgacgaagtgc-3′; Sox11-AS, 5′-tgaacaccaggtcggagaag-3′; mouse Bhlhb5: Bhlhb5-S, 5′-gttgcgcctcaacatcaac-3′; Bhlhb5-AS, 5′-acttttgcagaggctggac-3′; mouse Bcl11a: Bcl11a-S, 5′-gcatcaagctggagaaggag-3′; Bcl11a-AS, 5′-gagcttccatccgaaaactg-3′; mouse Gapdh: Gapdh-S, 5′-accacagtccatgccatcac-3′; Gapdh-AS, 5′-tccaccaccctgttgctgta-3′.

In situ hybridization

Digoxigenin- (DIG; Roche) labeled cRNA probes were synthesized for each gene, following the manufacturer's instructions. Cryosections were washed with PBS and fixed with 4% PFA. After fixation, sections were incubated in prehybridization solution (5× sodium chloride sodium citrate (SSC), 1% SDS, 50 μg/ml yeast transfer RNA, 50 μg/ml heparin in 50% formamide) at 70 °C for 1 h and hybridized with 500 ng/ml of DIG-labeled cRNA probes at 65 °C for 16 h. After three washes with wash solution 1 (5× SSC, 1% SDS in 50% formamide) and wash solution 3 (2× SSC in 50% formamide), sections were blocked with 10% normal sheep serum in TBST at room temperature for 1 h and then incubated with 1:1000 alkaline phosphatase-conjugated anti-DIG antibody (Roche) at 4 °C for 16 h. After four washes with TBST, hybridized probes were visualized with 5-bromo-4-chloro-3 indolylphosphate and nitro blue tetrazolium chloride.

Recombinant retrovirus construction and infection

Human *N-myc* and mouse *Hmga2* cDNAs were cloned into the expression vector pMYs, which contains an internal ribosome entry site followed by the region upstream of the *EGFP* gene (Morita et al., 2000). The Plat-E packaging cell line was transiently transfected with the retrovirus DNA by Trans-IT 293 (Mirus, Madison, WI, USA) (Morita et al., 2000). On the following day, the medium was replaced with N2/DMEM/F12/bFGF, and the cells were cultured in this medium for 1 day before virus was collected.

Fluorescence activated cell sorting

Virus-infected E11.5 NPCs were cultured for 4 days, after which GFP-labeled cells were sorted using a FACS Vantage (Becton Dickinson, Franklin Lakes, NJ, USA) at a flow rate of less than 1500 events/s; gating parameters were set by side and forward scatter to eliminate debris, dead and aggregated cells. After sorting, genomic DNA was extracted and used for bisulfite sequencing.

Bisulfite sequencing

Sodium bisulfite treatment of genomic DNA was performed using a Methylamp DNA Modification kit (Epigentek, Brooklyn, NY, USA), according to the manufacturer's instructions. The region in the *gfap* promoter containing the STAT-binding site of the bisulfite-treated genomic DNA was amplified by PCR using the following primers: GFmS (5′-GGGATTTATTAGGAGAATTTTAGAAGTAG-3′), GFmAS (5′-TCTACCCATACTTAAACTTCTAATATCTAC-3′). The PCR products were cloned into pT7Blue vector (Novagen, Madison, WI, USA) and at least 12 randomly selected clones were sequenced.

RESULTS

Preparation of NPCs from different developmental stages and comparison of their gene expression profiles by GeneChip analysis

E11.5 NPCs do not differentiate into astrocytes, even in the presence of the astrocyte-inducing cytokine LIF, in contrast to 4-day cultured E14.5 NPCs (Takizawa et al., 2001). As a first step toward identifying factors involved in the inhibition of astrocyte differentiation of NPCs at midgestation, we examined the gene expression profiles of E11.5 and E14.5 NPCs.

E11.5 and E14.5 NPCs were isolated from embryonic telencephalon and cultured as indicated in Fig. 1A. To evaluate the purity of NPCs in each cell population, the cells were stained with antibody against SOX2, an NPC marker (Graham et al., 2003). As shown in Fig. 1B and C, the majority of cells in both populations were positive for SOX2, indicating that NPCs were highly enriched. An Affymetrix mouse genome GeneChip array was chosen to compare expression profiles in the two populations, and we adopted the Percellome method to normalize gene expression from different samples (Kanno et al., 2006). The method enabled us to quantify mRNA molecules per cell based on the measurement of cell by adding a grade-dosed spike cocktail to the samples. We excluded genes whose transcript copy number was below six per cell. Scatter plots illustrating the differences between E11.5 and E14.5 NPCs are shown in Fig. 1D; 194 genes were expressed at >fivefold higher level in E11.5 NPCs than in E14.5 NPCs (Fig. 1D, light blue zone). Of these, 102 were known genes, and were classified by functional category (Fig. 1E). Since we wished to identify negative regulators of astrocyte differentiation, or factors involved in the epigenetic modification in midgestational NPCs, we focused on transcription-related genes (Fig. 1E, red). These 21 genes are listed in Table 1, and five (*N-myc*, *Hmga2*, *Bhlhb5*, *Sox11*, *Bcl11a*) were selected for further analysis because they have been reported to play roles in cell growth, differentiation, and chromatin remodeling in other types of stem cells (Sawai et al., 1990; Zhou et al., 1995; Saiki et al., 2000; Knoepfler et al., 2002; Brunelli et al., 2003; Sock et al., 2004).